

OAK RIDGE  
NATIONAL LABORATORY

MANAGED BY UT-BATTELLE  
FOR THE DEPARTMENT OF ENERGY

# **Quality Assurance Calculations to Support Use of HELIOS Version 1.6 for Plutonium Disposition Studies**

C. E. Sanders  
R. T. Primm III

## DOCUMENT AVAILABILITY

Reports produced after January 1, 1996, are generally available free via the U.S. Department of Energy (DOE) Information Bridge.

**Web site** <http://www.osti.gov/bridge>

Reports produced before January 1, 1996, may be purchased by members of the public from the following source.

National Technical Information Service

5285 Port Royal Road

Springfield, VA 22161

**Telephone** 703-605-6000 (1-800-553-6847)

**TDD** 703-487-4639

**Fax** 703-605-6900

**E-mail** [info@ntis.fedworld.gov](mailto:info@ntis.fedworld.gov)

**Web site** <http://www.ntis.gov/support/ordernowabout.htm>

Reports are available to DOE employees, DOE contractors, Energy Technology Data Exchange (ETDE) representatives, and International Nuclear Information System (INIS) representatives from the following source.

Office of Scientific and Technical Information

P.O. Box 62

Oak Ridge, TN 37831

**Telephone** 865-576-8401

**Fax** 865-576-5728

**E-mail** [reports@adonis.osti.gov](mailto:reports@adonis.osti.gov)

**Web site** <http://www.osti.gov/contact.html>

This report was prepared as an account of work sponsored by an agency of the United States government. Neither the United States government nor any agency thereof, nor any of their employees, makes any warranty, express or implied, or assumes any legal liability or responsibility for the accuracy, completeness, or usefulness of any information, apparatus, product, or process disclosed, or represents that its use would not infringe privately owned rights. Reference herein to any specific commercial product, process, or service by trade name, trademark, manufacturer, or otherwise, does not necessarily constitute or imply its endorsement, recommendation, or favoring by the United States government or any agency thereof. The views and opinions of authors expressed herein do not necessarily state or reflect those of the United States government or any agency thereof.

Computational Physics and Engineering Division (10)

## **Quality Assurance Calculations to Support Use of HELIOS Version 1.6 for Plutonium Disposition Studies**

**C. E. Sanders and R. T. Primm III**

Oak Ridge National Laboratory,  
P.O. Box 2008,  
Oak Ridge, TN 37831-6370

Date Published: April 2001

Prepared by the  
OAK RIDGE NATIONAL LABORATORY  
Oak Ridge, Tennessee 37831  
managed and operated by  
UT-Battelle, LLC  
for the  
U.S. DEPARTMENT OF ENERGY  
under contract DE-AC05-00OR22725



# CONTENTS

LIST OF FIGURES.....	v
LIST OF TABLES .....	vii
ACKNOWLEDGMENTS.....	ix
ABSTRACT .....	xi
1. INTRODUCTION.....	1
1.1. HELIOS – A Program for Performing Assembly Level Reactor Physics Calculations .....	1
1.2. Computer Code Changes from Version 1.4 to 1.6.....	2
1.3. Cross-Section Libraries – Changes from Version 1.4 to 1.6.....	2
2. PROCEDURE FOR COMPARISON OF VERSIONS 1.4 AND 1.6.....	9
3. QUAD CITIES BOILING-WATER-REACTOR (BWR) ASSEMBLY CONTAINING MIXED OXIDE (MOX) PINS AND LOW-ENRICHED URANIUM (LEU) PINS .....	11
4. ABB-CE MIXED OXIDE ASSEMBLY WITH 24 $\text{UO}_2\text{-ER}_2\text{O}_3$ RODS .....	21
5. WESTINGHOUSE $17 \times 17$ PRESSURIZED WATER REACTOR, MIXED OXIDE AND LOW-ENRICHED URANIUM (LEU) ASSEMBLIES.....	23
6. INFINITE ARRAYS OF VVER-1000 FUEL ASSEMBLIES .....	27
6.1. Variant 11, State 2, Burnup 60 MWd/kgU.....	27
6.2. Variant 12, State 2, Burnup 60 MWd/kgU.....	32
6.3. Variant 14, State 6, Burnup 60 MWd/kgU.....	37
6.4. Variant 20, State 8.....	39
6.5. Conclusions .....	40
7. DESTRUCTIVELY ASSAYED VVER-1000 LEU ASSEMBLY .....	41
8. CONCLUSIONS .....	43
9. REFERENCES.....	45



## LIST OF FIGURES

<b><u>Figure</u></b>	<b><u>Page</u></b>
1. Cell relative fission rate distribution is relative to the total corresponding fission rate for the entire assembly. Variant 11, State 2, 60 Burnup MWd/kgU.....	31
2. Cell relative fission rate distribution is relative to the total corresponding fission rate for the entire assembly. Variant 12, State 2, 60 Burnup MWd/kgU.....	36
3. Cell relative fission rate distribution is relative to the total corresponding fission rate for the entire assembly. Variant 14, State 6, Burnup 60 MWd/kgU.....	37





# LIST OF TABLES

<b><u>Table</u></b>	<b><u>Page</u></b>
1. HELIOS-34 group library structure .....	3
2. HELIOS-89 group library structure .....	4
3. HELIOS-190 group library structure .....	5
4. HELIOS-45 group library structure .....	7
5. Computational problem set .....	10
6. Characteristics of pins in assembly GEB-161 .....	11
7. Pin D3 of GEB-161 (at 11,722 MWd/kgU) .....	12
8. Pin D5 of GEB-161 (at 11,722 MWd/kgU) .....	13
9. Pin E3 of GEB-161 (at 11,722 MWd/kgU) .....	14
10. Pin E4 of GEB-161 (at 11,722 MWd/kgU) .....	15
11. Pin C2 of GEB-161 (at 11,722 MWd/kgU) .....	16
12. Pin D1 of GEB-161 (at 11,722 MWd/kgU) .....	17
13. Pin D2 of GEB-161 (at 11,722 MWd/kgU) .....	18
14. Pin F6 of GEB-161 (at 11,722 MWd/kgU) .....	19
15. Pin G1 of GEB-161 (at 11,722 MWd/kgU) .....	20
16. Comparison of multiplication factors for an ABB-CE MOX assembly .....	22
17. Comparison of multiplication factors for Westinghouse $17 \times 17$ LEU assembly .....	24
18. Comparison of multiplication factors for Westinghouse $17 \times 17$ MOX assembly .....	25
19. Values of $k_{eff}$ , $k_0$ , and migration area .....	27
20. Cell macroscopic cross sections, flux, and flux ratios .....	27
21. Cell relative absorption reaction rates .....	28
22. Fuel-averaged microscopic absorption cross section .....	29
23. Cell relative production rates .....	29
24. Fuel-averaged microscopic production cross section .....	30
25. Values of $k_{eff}$ , $k_0$ , and migration area .....	32
26. Cell macroscopic cross sections, flux, and flux ratios .....	32
27. Cell relative absorption reaction rates .....	33
28. Fuel-averaged microscopic absorption cross section .....	34

29.	Cell relative production rates .....	34
30.	Fuel-averaged microscopic production cross section.....	35
31.	Delayed neutron fraction, effective delayed neutron fraction, and prompt neutron lifetime .....	40
32.	Balakovo-3, Sample 581 .....	42

## **ACKNOWLEDGMENTS**

This work was sponsored by the Office of Fissile Materials Disposition of the Office of Nuclear Nonproliferation of the National Nuclear Security Administration of the United States Department of Energy. The authors are grateful to Brian D. Murphy and Jess C. Gehin for their careful review of this document. In addition, the authors are thankful to Willena C. Carter for preparing this document.



## ABSTRACT

In mid-2000, the Reactor Physics Group at Oak Ridge National Laboratory (ORNL) purchased a new version of the HELIOS, assembly-level reactor physics computer program (version 1.6). While the authors of the HELIOS program had performed validation and verification studies and compared results to versions 1.4 and 1.5, geometries and materials similar to those expected for mixed oxide fuel (MOX) in Russian water-water energetic reactors (VVER) had not been investigated. The studies reported in this document are a program-specific supplement to the work performed by the computer program authors and are performed to comply with quality assurance procedures of the Reactor Physics Group of ORNL.

There were two goals for these studies. First, quantify the differences in nuclide inventories or other physics parameters, such as multiplication factors, due to the use of version 1.6 instead of 1.4. Second, determine if results from the version 1.6 design library (a 45 energy group library) differed significantly (meaning absolute value of the difference greater than or equal to 1%) from values obtained with the 190 group master library.

Changes in nuclide inventories and multiplication factors are dependent on the system studied (whether U.S. or Russian reactors) and the type of fuel (whether low-enriched or mixed oxide). For selected actinides, the differences between the design library for version 1.4 and the master library for version 1.6 can be as high as 15%.



# 1. INTRODUCTION

The Fissile Materials Disposition Program (FMDP) has as one of its goals the transformation of weapons-usable plutonium into mixed oxide fuel (MOX) and the irradiation of that fuel in Russian pressurized water reactors (VVERs). A description of the reactor physics analyses required to support the program is provided in Ref. 1. A series of verification and validation studies for the computer programs and data to be used in the analyses of VVERs are referenced in that document. All of these studies, along with subsequent assembly design studies, were performed with version 1.4 of the HELIOS program (and its associated libraries).

In mid-2000, the FMDP purchased a new version of the HELIOS program (1.6). While the authors of the HELIOS program had performed validation and verification studies and compared results to versions 1.4 and 1.5, geometries and materials similar to those expected for MOX in VVERs had not been investigated. The studies reported in this document represent a program-specific supplement to the work performed by the computer program authors and are performed to comply with quality assurance procedures of the Reactor Physics Group of Oak Ridge National Laboratory.

There were two goals for these studies. First, quantify the differences in nuclide inventories or other physics parameters (e.g., such as multiplication factors) due to the use of version 1.6 instead of 1.4. Second, determine if results from the version 1.6 design library (45-energy group library) differed significantly (meaning absolute value of the difference greater than or equal to 1%) from values obtained with the 190 group master library. Upon examining version 1.6, the first goal was found not to be literally achievable as the group structure of the design library had been changed from 34 to 45 groups. Nevertheless, comparisons between 34 and 45-group calculations are made and the results of this first study can be used, when needed, to compare calculations already completed and documented, to new calculations currently being performed or to be performed in the future. The results of the second study can be used to identify biases in design calculations and to identify specific areas of study where the design library may not be sufficiently accurate.

## 1.1. HELIOS – A Program for Performing Assembly Level Reactor Physics Calculations

“HELIOS is a neutron and gamma transport code for lattice burnup in general two-dimensional geometry. ... HELIOS performs resonance shielding calculations for nuclides with resolved resonance data. ... the transport method of HELIOS is called the CCCP method, because it is based on current coupling and collision probabilities. It is actually first-flight probability because transmission and escape probabilities are included. For reasons of tradition, collision probabilities are retained in the solution method acronym. The system to be calculated is made up of space elements that are coupled by interface currents with each other and with the boundaries, while the properties of each space element – its responses to sources and in-currents – are obtained from (collision probabilities).”<sup>2</sup>

## 1.2. Computer Code Changes from Version 1.4 to 1.6

The HELIOS program was modified to add the (n, 2n) and (n, 3n) effects to the gain rate due to capture. In the depletion portion of the calculation, both the loss and gain due to the (n, 2n) and (n, 3n) reactions were included. These changes cause a reactivity gain with burnup that varies from case to case. In some cases in the Studsvik reports, it is as large as +325 pcm (percent milli-k) at 44,000 MWd/MT.

Some minor errors in the program were corrected. These include: iteration errors for cases with very little thermal flux in the system examined, increase in convergence speed for the calculation of the resonance integral cross-section values and various clerical corrections involving reporting the date on which the calculation was performed. None of these should have had an impact on calculations performed for the FMDP with previous versions of HELIOS.

## 1.3. Cross-Section Libraries – Changes from Version 1.4 to 1.6

The NJOY<sup>3</sup> code system and the ENDF/B-VI<sup>4</sup> data files were the genesis of the production procedure for the HELIOS libraries. An integral transport theory program, RABBLE, was used to generate cross-section tables for the resonance region. RABBLE data were based on the explicit representation of a pin cell rather than the spatial approximation contained in the GROUPE module of the NJOY system.

For Version 1.4, a 190 neutron group, 48-gamma group master data base (library) was generated from ENDF/B-VI. The data base contains a spectrum which can be used to collapse the library to any group structure which is a subset of the master. Scandpower provides “condensed” libraries having 34 and 89 energy groups which were generated using the spectrum contained in the master data base. The group boundaries for the 34, 89, and 190-group HELIOS libraries are provided in Tables 1–3.

Two cross-section libraries are distributed with version 1.6. The number of energy groups in the “broad” group library was increased from 34 to 45 (a 35<sup>th</sup> group had been added to the library with the distribution of version 1.5). Groups 1–9 are designated “fast” energy groups; groups 9–25 are the resonance range, and groups 23–45 allow for upscatter and thus are designated the thermal range. The 89-group library (modified to 90 groups in version 1.5) is not distributed with version 1.6. Two versions of each library – 45 and 190 groups – are distributed. The only difference between them is that one version of each has an adjustment applied to the <sup>238</sup>U resonance integral – a reduction of 3.4% based on the results of verification and validation studies. Table 4 describes the group boundaries for the 45-group HELIOS library. All of the version 1.6 calculations reported in this document were performed with libraries having the adjusted <sup>238</sup>U resonance integral.

In addition to modifying the group structure of the design library, several minor changes were made to the libraries. <sup>238</sup>Pu and <sup>241</sup>Am have improved resonance integral cross sections. The 1.06 eV resonance of <sup>240</sup>Pu has been shielded with a background cross section leading to slightly (1%) greater <sup>240</sup>Pu concentrations at high burnups. Delayed neutron fraction values were revised for almost all actinides. Two fission gas isotopes, <sup>128</sup>Xe and <sup>130</sup>Xe, have been included in



the burnup chains. Lastly, an error in the NJOY code used to process the ENDF/B-VI data was corrected and all of the thermal data for all nuclides were regenerated. An increased accuracy in the fuel temperature coefficient for Pu-bearing fuels resulted from the NJOY correction.

**Table 1. HELIOS-34 group library structure**

Group number	Upper energy group limits (eV)	Group number	Upper energy group limits (eV)	Group number	Upper energy group limits (eV)	Group number	Upper energy group limits (eV)
1	2.000E+07	11	4.785E+01	21	1.099E+00	31	5.692E-02
2	3.679E+06	12	2.902E+01	22	1.014E+00	32	4.275E-02
3	1.353E+06	13	1.371E+01	23	9.506E-01	33	3.061E-02
4	4.979E+05	14	8.315E+00	24	6.251E-01	34	1.240E-02
5	1.832E+05	15	6.476E+00	25	3.577E-01		1.0E-5
6	6.738E+04	16	5.043E+00	26	2.705E-01		
7	9.119E+03	17	3.928E+00	27	1.844E-01		
8	2.035E+03	18	2.382E+00	28	1.457E-01		
9	1.301E+02	19	1.855E+00	29	1.116E-01		
10	7.889E+01	20	1.308E+00	30	8.197E-02		

**Table 2. HELIOS-89 group library structure**

Group number	Upper energy group limits (eV)	Group number	Upper energy group limits (eV)	Group number	Upper energy group limits (eV)	Group number	Upper energy group limits (eV)
1	2.000E+07	26	5.531E+03	51	1.855E+00	76	1.523E-01
2	7.408E+06	27	3.355E+03	52	1.726E+00	77	1.457E-01
3	6.065E+06	28	2.035E+03	53	1.595E+00	78	1.116E-01
4	4.493E+06	29	1.234E+03	54	1.457E+00	79	8.197E-02
5	3.679E+06	30	7.485E+02	55	1.308E+00	80	6.700E-02
6	2.725E+06	31	4.540E+02	56	1.166E+00	81	5.692E-02
7	2.231E+06	32	2.754E+02	57	1.099E+00	82	5.000E-02
8	1.827E+06	33	1.670E+02	58	1.072E+00	83	4.275E-02
9	1.353E+06	34	1.301E+02	59	1.062E+00	84	3.550E-02
10	1.003E+06	35	1.013E+02	60	1.053E+00	85	3.061E-02
11	8.208E+05	36	7.889E+01	61	1.043E+00	86	2.049E-02
12	6.081E+05	37	6.144E+01	62	1.014E+00	87	1.240E-02
13	4.979E+05	38	4.785E+01	63	9.506E-01	88	6.325E-03
14	3.688E+05	39	3.727E+01	64	7.821E-01	89	2.277E-03
15	3.020E+05	40	2.902E+01	65	6.251E-01		1.0E-5
16	2.237E+05	41	2.260E+01	66	5.032E-01		
17	1.832E+05	42	1.760E+01	67	4.170E-01		
18	1.500E+05	43	1.371E+01	68	3.577E-01		
19	1.111E+05	44	1.068E+01	69	3.206E-01		
20	8.652E+04	45	8.315E+00	70	3.011E-01		
21	6.738E+04	46	6.476E+00	71	2.907E-01		
22	4.087E+04	47	5.043E+00	72	2.705E-01		
23	2.479E+04	48	3.928E+00	73	2.510E-01		
24	1.503E+04	49	3.059E+00	74	2.277E-01		
25	9.119E+03	50	2.382E+00	75	1.844E-01		

**Table 3. HELIOS-190 group library structure**

Group number	Upper energy group limits (eV)	Group number	Upper energy group limits (eV)	Group number	Upper energy group limits (eV)	Group number	Upper energy group limits (eV)
1	2.000E+07	26	1.572E+06	51	4.087E+04	76	2.035E+03
2	1.700E+07	27	1.353E+06	52	3.607E+04	77	1.796E+03
3	1.492E+07	28	1.165E+06	53	3.183E+04	78	1.585E+03
4	1.338E+07	29	1.054E+06	54	2.809E+04	79	1.398E+03
5	1.200E+07	30	1.003E+06	55	2.606E+04	80	1.234E+03
6	1.000E+07	31	8.208E+05	56	2.479E+04	81	1.089E+03
7	8.825E+06	32	7.065E+05	57	2.187E+04	82	9.611E+02
8	7.788E+06	33	6.393E+05	58	1.930E+04	83	8.482E+02
9	7.408E+06	34	6.081E+05	59	1.704E+04	84	7.485E+02
10	6.065E+06	35	4.979E+05	60	1.503E+04	85	6.606E+02
11	5.220E+06	36	4.285E+05	61	1.327E+04	86	5.829E+02
12	4.724E+06	37	3.877E+05	62	1.171E+04	87	5.144E+02
13	4.493E+06	38	3.688E+05	63	1.033E+04	88	4.540E+02
14	4.066E+06	39	3.020E+05	64	9.119E+03	89	4.006E+02
15	3.679E+06	40	2.599E+05	65	8.047E+03	90	3.536E+02
16	3.166E+06	41	2.352E+05	66	7.102E+03	91	3.120E+02
17	2.865E+06	42	2.237E+05	67	6.267E+03	92	2.754E+02
18	2.725E+06	43	1.832E+05	68	5.531E+03	93	2.430E+02
19	2.466E+06	44	1.500E+05	69	4.881E+03	94	2.144E+02
20	2.365E+06	45	1.426E+05	70	4.307E+03	95	1.893E+02
21	2.346E+06	46	1.291E+05	71	3.801E+03	96	1.670E+02
22	2.231E+06	47	1.111E+05	72	3.355E+03	97	1.474E+02
23	2.019E+06	48	8.652E+04	73	2.960E+03	98	1.301E+02
24	1.827E+06	49	6.738E+04	74	2.613E+03	99	1.148E+02
25	1.738E+06	50	5.247E+04	75	2.306E+03	100	1.013E+02

**Table 3 (continued)**

Group number	Upper energy group limits (eV)	Group number	Upper energy group limits (eV)	Group number	Upper energy group limits (eV)	Group number	Upper energy group limits (eV)
101	8.940E+01	126	4.451E+00	151	9.920E-01	176	1.116E-01
102	7.889E+01	127	3.928E+00	152	9.710E-01	177	8.197E-02
103	6.962E+01	128	3.466E+00	153	9.506E-01	178	6.700E-02
104	6.144E+01	129	3.059E+00	154	9.100E-01	179	5.692E-02
105	5.422E+01	130	2.700E+00	155	8.764E-01	180	5.000E-02
106	4.785E+01	131	2.382E+00	156	8.337E-01	181	4.275E-02
107	4.223E+01	132	2.102E+00	157	7.821E-01	182	3.550E-02
108	3.727E+01	133	1.855E+00	158	7.300E-01	183	3.061E-02
109	3.289E+01	134	1.790E+00	159	6.700E-01	184	2.550E-02
110	2.902E+01	135	1.726E+00	160	6.251E-01	185	2.049E-02
111	2.561E+01	136	1.659E+00	161	5.700E-01	186	1.240E-02
112	2.260E+01	137	1.595E+00	162	5.300E-01	187	6.325E-03
113	1.995E+01	138	1.525E+00	163	5.032E-01	188	2.277E-03
114	1.760E+01	139	1.457E+00	164	4.500E-01	189	7.602E-04
115	1.554E+01	140	1.381E+00	165	4.170E-01	190	2.540E-04
116	1.371E+01	141	1.308E+00	166	3.577E-01		1.0E-5
117	1.210E+01	142	1.235E+00	167	3.206E-01		
118	1.068E+01	143	1.166E+00	168	3.011E-01		
119	9.422E+00	144	1.125E+00	169	2.907E-01		
120	8.315E+00	145	1.099E+00	170	2.705E-01		
121	7.338E+00	146	1.072E+00	171	2.510E-01		
122	6.868E+00	147	1.062E+00	172	2.277E-01		
123	6.476E+00	148	1.053E+00	173	1.844E-01		
124	5.715E+00	149	1.043E+00	174	1.523E-01		
125	5.043E+00	150	1.014E+00	175	1.457E-01		

**Table 4. HELIOS-45 group library structure**

Group	Lower limit (eV)
0	2.0000E+07 (upper limit)
1	6.0653E+06
2	3.6788E+06
3	2.2313E+06
4	1.3534E+06
5	8.2085E+05
6	4.9787E+05
7	1.8316E+05
8	6.7379E+04
9	9.1188E+03
10	2.0347E+03
11	1.3007E+02
12	78.893
13	47.851
14	29.023
15	13.710
16	12.099
17	8.3153
18	7.3382
19	6.476
20	5.715
21	5.0435
22	4.4509
23	3.9279
24	2.3824
25	1.8554
26	1.4574
27	1.2351
28	1.1254

**Table 4 (continued)**

Group	Lower limit (eV)
29	1.0722
30	1.0137
31	0.971
32	0.910
33	0.78208
34	0.62506
35	0.35767
36	0.27052
37	0.18443
38	0.14572
39	0.11157
40	0.081968
41	0.056922
42	0.042755
43	0.030613
44	0.012396
45	1.0E-04
	1.0E-05

## **2. PROCEDURE FOR COMPARISON OF VERSIONS 1.4 AND 1.6**

Version 1.6 was installed by the computer system manager on the computer hardware according to instructions provided by the code vendor (Studsvik/Scandpower). Sample problems provided by the vendor were executed and compared to vendor results for these problems. The results were in perfect agreement.

A set of computational problems was selected to link the new version of the code to past verification and validation studies performed under prior programmatic funding. The set is presented in Table 5. Datasets for these cases had already been prepared and stored in the Reactor Physics Group's quality assurance (QA) files. No new models were developed for this study. Computational results from these existing datasets have been published in a format that required a minimum of two technical reviewers (see references in Table 5). Cases 1 and 5 are physical measurements whereas cases 2–4 are computational benchmarks.

The lead author, being familiar with the HELIOS program, was selected by the Reactor Physics Group leader (second author) to calculate the set identified in Table 5. Succeeding sections of this report present the comparisons between calculations performed with Versions 1.6 and 1.4.

**Table 5. Computational problem set**

Case	Description	Reference	Case identifier in reference	Parameters for comparison
1	Quad Cities BWR assembly containing MOX pins and LEU pins some with Gd	ORNL/TM-13567 (Ref. 5)	Appendix C	Appendix D, compare to calculated atom density columns
2	ABB-CE MOX assembly with 24 $\text{UO}_2\text{-Er}_2\text{O}_3$ rods	ORNL/SUB/99-19XSY063V-1 (Ref. 6)	MOX assembly with 24 $\text{UO}_2\text{-Er}_2\text{O}_3$ rods	Table 1 and Figure 1
3	Westinghouse $17 \times 17$ PWR, MOX and LEU	ORNL/SUB/99-19XSY062V-1 (Ref. 7)	1. Table II.a, hmlwh89g.inp, (MOX) 2. Table II.a, huh128i.inp (LEU)	Table XIII
4	VVER-1000 - infinite array of high burnup LEU; infinite array of high burnup MOX; infinite array of a mixture of MOX and LEU with burnup at room temp.; infinite array of a mixture of MOX and LEU under accident conditions	ORNL/TM-1999/78 (Ref. 8)	[format is variant, state burnup] V11S2(60), V12S2(60), V14S6(60), V20S8	Various tables in ORNL/TM-1999/78 that reference these states
5	VVER-1000 - LEU assembly	ORNL/TM-1999/168 (Ref. 9)	Sample 581	Table 6 and Table 1



### 3. QUAD CITIES BOILING-WATER-REACTOR (BWR) ASSEMBLY CONTAINING MIXED OXIDE (MOX) PINS AND LOW-ENRICHED URANIUM (LEU) PINS

During the 1970s, test assemblies containing both LEU and MOX pins were irradiated in the Quad Cities BWR. A description of the assemblies and the results of HELIOS version 1.4 calculations are documented in Ref. 5. The assembly was a square pitch, seven pin by seven pin configuration. The calculations reported in Ref. 5 were performed with the 34-energy group unadjusted library.

The original input files for the calculations in Ref. 5 were recovered and executed with the sole change being that the 'Path' operator had been commented out and replaced with a burnup sequence that was not applicable for the comparisons reported. The lead author changed the 'Path' operator back to its original value (11,722 MWd/kgU) that is suitable for these comparisons.

Some of the characteristics of the pins in assembly GEB-161 are given in Table 6. Tables 7–15 provide the results of the version 1.6 calculations and also provide values reported in Ref. 5.

**Table 6. Characteristics of pins in assembly GEB-161**

Pin Id	Type	<sup>235</sup> U enrichment in U (%)	Fissile Pu (wt %)	Gd <sub>2</sub> O <sub>3</sub> (wt %) in fuel
D3	Annular	0.72	2.34	0
D5	Solid	0.72	3.52	0
E3	Solid	0.72	2.14	0
E4	Annular	0.72	3.62	0
C2	Solid	2.56	0	0
D1	Solid	1.94	0	0
D2	Solid	3.30	0	0
F6	Solid	2.56	0	2.5
G1	Solid	1.69	0	0

**Table 7. Pin D3 of GEB-161 (at 11,722 MWd/kgU)**

Nuclide	HELIOS-1.4 34-group cross- section library	HELIOS-1.6 45-group cross- section library	HELIOS-1.6 190-group cross- section library	Version 1.4 – 45 groups	Version 1.4 – 190 groups
	Atom density (atoms/barn-cm)	Atom density (atoms/barn-cm)	Atom density (atoms/barn-cm)	%	%
<sup>235</sup> U	1.017E-04	1.0122E-04	1.0143E-04	0.5	0.3
<sup>236</sup> U	7.288E-06	7.3494E-06	7.2786E-06	-0.8	0.1
<sup>238</sup> U	1.910E-02	1.9101E-02	1.9101E-02	0.0	0.0
<sup>237</sup> Np	8.110E-07	8.2190E-07	8.2416E-07	-1.3	-1.6
<sup>239</sup> Pu	2.538E-04	2.5144E-04	2.5161E-04	0.9	0.9
<sup>240</sup> Pu	1.461E-04	1.4592E-04	1.4607E-04	0.1	0.0
<sup>241</sup> Pu	4.970E-05	4.8568E-05	4.8356E-05	2.3	2.7
<sup>242</sup> Pu	1.321E-05	1.3291E-05	1.3191E-05	-0.6	0.1
<sup>241</sup> Am	2.085E-06	2.0452E-06	2.0476E-06	1.9	1.8
<sup>243</sup> Am	1.609E-06	1.5165E-06	1.5731E-06	5.7	2.2
<sup>242</sup> Cm	2.516E-07	2.5161E-07	2.4811E-07	0.0	1.4
<sup>243</sup> Cm + <sup>244</sup> Cm	2.392E-07	2.2937E-07	2.3769E-07	4.1	0.6
<sup>145</sup> Nd	8.135E-06	8.0990E-06	8.0788E-06	0.4	0.7
<sup>146</sup> Nd	7.108E-06	7.0800E-06	7.0642E-06	0.4	0.6
<sup>148</sup> Nd	4.518E-06	4.4979E-06	4.4874E-06	0.4	0.7

**Table 8. Pin D5 of GEB-161 (at 11,722 MWd/kgU)**

Nuclide	HELIOS-1.4	HELIOS-1.6	HELIOS-1.6	Version 1.4 – 45 groups	Version 1.4 – 190 groups
	34-group cross- section library	45-group cross- section library	190-group cross- section library		
	Atom density (atoms/barn·cm)	Atom density (atoms/barn·cm)	Atom density (atoms/barn·cm)		
<sup>235</sup> U	1.227E-04	1.2226E-04	1.2244E-04	0.4	0.2
<sup>236</sup> U	6.448E-06	6.5107E-06	6.4330E-06	-1.0	0.2
<sup>238</sup> U	2.092E-02	2.0922E-02	2.0922E-02	0.0	0.0
<sup>237</sup> Np	8.791E-07	8.8502E-07	8.8667E-07	-0.7	-0.9
<sup>239</sup> Pu	5.087E-04	5.0506E-04	5.0645E-04	0.7	0.4
<sup>240</sup> Pu	1.556E-04	1.5538E-04	1.5493E-04	0.1	0.4
<sup>241</sup> Pu	4.860E-05	4.7392E-05	4.7204E-05	2.5	2.9
<sup>242</sup> Pu	6.620E-06	6.6995E-06	6.6569E-06	-1.2	-0.6
<sup>241</sup> Am	2.000E-06	1.9580E-06	1.9556E-06	2.1	2.2
<sup>243</sup> Am	7.662E-07	7.3541E-07	7.5409E-07	4.0	1.6
<sup>242</sup> Cm	1.720E-07	1.7353E-07	1.7268E-07	-0.9	-0.4
<sup>243</sup> Cm+	1.020E-07	9.9662E-08	1.0212E-07	2.3	-0.1
<sup>244</sup> Cm					
<sup>145</sup> Nd	8.729E-06	8.7084E-06	8.6695E-06	0.2	0.7
<sup>146</sup> Nd	7.580E-06	7.5664E-06	7.5346E-06	0.2	0.6
<sup>148</sup> Nd	4.848E-06	4.8367E-06	4.8157E-06	0.2	0.7

**Table 9. Pin E3 of GEB-161 (at 11,722 MWd/kgU)**

	HELIOS-1.4 34-group cross- section library	HELIOS-1.6 45-group cross- section library	HELIOS-1.6 190-group cross- section library	Version 1.4 – 45 groups	Version 1.4 – 190 groups
Nuclide	Atom density (atoms/barn-cm)	Atom density (atoms/barn-cm)	Atom density (atoms/barn-cm)	%	%
<sup>235</sup> U	1.142E-04	1.1364E-04	1.1385E-04	0.5	0.3
<sup>236</sup> U	7.895E-06	7.9576E-06	7.8812E-06	-0.8	0.2
<sup>238</sup> U	2.118E-02	2.1184E-02	2.1184E-02	0.0	0.0
<sup>237</sup> Np	8.876E-07	8.9839E-07	9.0069E-07	-1.2	-1.5
<sup>239</sup> Pu	2.706E-04	2.6800E-04	2.6810E-04	1.0	0.9
<sup>240</sup> Pu	1.481E-04	1.4795E-04	1.4808E-04	0.1	0.0
<sup>241</sup> Pu	5.077E-05	4.9583E-05	4.9368E-05	2.3	2.8
<sup>242</sup> Pu	1.311E-05	1.3205E-05	1.3108E-05	-0.7	0.0
<sup>241</sup> Am	2.141E-06	2.0990E-06	2.1006E-06	2.0	1.9
<sup>243</sup> Am	1.620E-06	1.5235E-06	1.5814E-06	6.0	2.4
<sup>242</sup> Cm	2.505E-07	2.5056E-07	2.4731E-07	0.0	1.3
<sup>243</sup> Cm+ <sup>244</sup> Cm	2.414E-07	2.3106E-07	2.3961E-07	4.3	0.7
<sup>145</sup> Nd	8.252E-06	8.2183E-06	8.1989E-06	0.4	0.6
<sup>146</sup> Nd	7.201E-06	7.1748E-06	7.1600E-06	0.4	0.6
<sup>148</sup> Nd	4.570E-06	4.5508E-06	4.5409E-06	0.4	0.6

**Table 10. Pin E4 of GEB-161 (at 11,722 MWd/kgU)**

Nuclide	HELIOS-1.4	HELIOS-1.6	HELIOS-1.6	Version 1.4 – 45 groups	Version 1.4 – 190 groups
	34-group cross- section library	45-group cross- section library	190-group cross- section library		
	Atom density (atoms/barn·cm)	Atom density (atoms/barn·cm)	Atom density (atoms/barn·cm)		
				%	%
<sup>235</sup> U	1.099E-04	1.0953E-04	1.0969E-04	0.3	0.2
<sup>236</sup> U	5.948E-06	6.0086E-06	5.9387E-06	-1.0	0.2
<sup>238</sup> U	1.888E-02	1.8888E-02	1.8889E-02	0.0	0.0
<sup>237</sup> Np	7.950E-07	8.0152E-07	8.0321E-07	-0.8	-1.0
<sup>239</sup> Pu	4.626E-04	4.5888E-04	4.6009E-04	0.8	0.5
<sup>240</sup> Pu	1.462E-04	1.4600E-04	1.4562E-04	0.1	0.4
<sup>241</sup> Pu	4.607E-05	4.4991E-05	4.4832E-05	2.3	2.7
<sup>242</sup> Pu	6.398E-06	6.4710E-06	6.4324E-06	-1.1	-0.5
<sup>241</sup> Am	1.875E-06	1.8380E-06	1.8369E-06	2.0	2.0
<sup>243</sup> Am	7.351E-07	7.0777E-07	7.2516E-07	3.7	1.4
<sup>242</sup> Cm	1.665E-07	1.6794E-07	1.6700E-07	-0.9	-0.3
<sup>243</sup> Cm+	9.807E-08	9.6132E-08	9.8402E-08	2.0	-0.3
<sup>244</sup> Cm					
<sup>145</sup> Nd	8.308E-06	8.2929E-06	8.2591E-06	0.2	0.6
<sup>146</sup> Nd	7.221E-06	7.2108E-06	7.1832E-06	0.1	0.5
<sup>148</sup> Nd	4.620E-06	4.6114E-06	4.5932E-06	0.2	0.6

**Table 11. Pin C2 of GEB-161 (at 11,722 MWd/kgU)**

Nuclide	HELIOS-1.4	HELIOS-1.6	HELIOS-1.6	Version 1.4 – 45 groups	Version 1.4 – 190 groups
	34-group cross- section library	45-group cross- section library	190-group cross- section library		
	Atom density (atoms/barn·cm)	Atom density (atoms/barn·cm)	Atom density (atoms/barn·cm)		
<sup>235</sup> U	3.433E-04	3.4045E-04	3.4096E-04	0.8	0.7
<sup>236</sup> U	4.220E-05	4.2498E-05	4.2317E-05	-0.7	-0.3
<sup>238</sup> U	2.227E-02	2.2271E-02	2.2272E-02	0.0	0.0
<sup>237</sup> Np	1.630E-06	1.6794E-06	1.6795E-06	-3.0	-3.0
<sup>239</sup> Pu	7.018E-05	6.7864E-05	6.7106E-05	3.3	4.4
<sup>240</sup> Pu	1.735E-05	1.6622E-05	1.6393E-05	4.2	5.5
<sup>241</sup> Pu	5.363E-06	5.0923E-06	5.2673E-06	5.0	1.8
<sup>242</sup> Pu	6.850E-07	6.5250E-07	6.8912E-07	4.7	-0.6
<sup>241</sup> Am	1.003E-07	9.4394E-08	9.9307E-08	5.9	1.0
<sup>243</sup> Am	3.748E-08	3.5648E-08	3.8825E-08	4.9	-3.6
<sup>242</sup> Cm	1.257E-08	1.1822E-08	1.2372E-08	6.0	1.6
<sup>243</sup> Cm+ <sup>244</sup> Cm	2.789E-09	2.6786E-09	2.9347E-09	4.0	-5.2
<sup>145</sup> Nd	1.001E-05	1.0047E-05	1.0038E-05	-0.4	-0.3
<sup>146</sup> Nd	8.447E-06	8.4798E-06	8.4758E-06	-0.4	-0.3
<sup>148</sup> Nd	4.747E-06	4.7575E-06	4.7551E-06	-0.2	-0.2

**Table 12. Pin D1 of GEB-161 (at 11,722 MWd/kgU)**

Nuclide	HELIOS-1.4	HELIOS-1.6	HELIOS-1.6	Version 1.4 – 45 groups	Version 1.4 – 190 groups
	34-group cross- section library	45-group cross- section library	190-group cross- section library		
	Atom density (atoms/barn-cm)	Atom density (atoms/barn-cm)	Atom density (atoms/barn-cm)		
<sup>235</sup> U	2.159E-04	2.1308E-04	2.1327E-04	1.3	1.2
<sup>236</sup> U	3.793E-05	3.8195E-05	3.8090E-05	-0.7	-0.4
<sup>238</sup> U	2.239E-02	2.2392E-02	2.2393E-02	0.0	0.0
<sup>237</sup> Np	1.585E-06	1.6469E-06	1.6503E-06	-3.9	-4.1
<sup>239</sup> Pu	6.820E-05	6.6350E-05	6.5688E-05	2.7	3.7
<sup>240</sup> Pu	2.171E-05	2.0936E-05	2.0688E-05	3.6	4.7
<sup>241</sup> Pu	6.829E-06	6.5378E-06	6.7170E-06	4.3	1.6
<sup>242</sup> Pu	1.204E-06	1.1576E-06	1.2156E-06	3.9	-1.0
<sup>241</sup> Am	1.278E-07	1.2139E-07	1.2686E-07	5.0	0.7
<sup>243</sup> Am	7.224E-08	6.9417E-08	7.5080E-08	3.9	-3.9
<sup>242</sup> Cm	2.051E-08	1.9479E-08	2.0258E-08	5.0	1.2
<sup>243</sup> Cm+	6.053E-09	5.8708E-09	6.3951E-09	3.0	-5.7
<sup>244</sup> Cm					
<sup>145</sup> Nd	9.946E-06	9.9716E-06	9.9771E-06	-0.3	-0.3
<sup>146</sup> Nd	8.550E-06	8.5795E-06	8.5881E-06	-0.3	-0.4
<sup>148</sup> Nd	4.834E-06	4.8410E-06	4.8460E-06	-0.1	-0.2

**Table 13. Pin D2 of GEB-161 (at 11,722 MWd/kgU)**

Nuclide	HELIOS-1.4	HELIOS-1.6	HELIOS-1.6	Version 1.4 – 45 groups	Version 1.4
	34 -group cross- section library	45-group cross- section library	190-group cross- section library		– 190 groups
	Atom density (atoms/barn·cm)	Atom density (atoms/barn·cm)	Atom density (atoms/barn·cm)		%
<sup>235</sup> U	4.754E-04	4.7237E-04	4.7303E-04	0.6	0.5
<sup>236</sup> U	4.994E-05	5.0271E-05	5.0036E-05	–0.7	–0.2
<sup>238</sup> U	2.210E-02	2.2107E-02	2.2108E-02	0.0	0.0
<sup>237</sup> Np	1.795E-06	1.8328E-06	1.8321E-06	–2.1	–2.1
<sup>239</sup> Pu	7.206E-05	6.9274E-05	6.8476E-05	3.9	5.0
<sup>240</sup> Pu	1.561E-05	1.4914E-05	1.4699E-05	4.5	5.8
<sup>241</sup> Pu	4.865E-06	4.5965E-06	4.7808E-06	5.5	1.7
<sup>242</sup> Pu	5.289E-07	5.0210E-07	5.3310E-07	5.1	–0.8
<sup>241</sup> Am	9.068E-08	8.4923E-08	8.9792E-08	6.3	1.0
<sup>243</sup> Am	2.823E-08	2.6726E-08	2.9325E-08	5.3	–3.9
<sup>242</sup> Cm	1.011E-08	9.4756E-09	9.9745E-09	6.3	1.3
<sup>243</sup> Cm+	2.021E-09	1.9333E-09	2.1346E-09	4.3	–5.6
<sup>244</sup> Cm					
<sup>145</sup> Nd	1.111E-05	1.1147E-05	1.1133E-05	–0.3	–0.2
<sup>146</sup> Nd	9.293E-06	9.3330E-06	9.3257E-06	–0.4	–0.4
<sup>148</sup> Nd	5.193E-06	5.2073E-06	5.2029E-06	–0.3	–0.2



**Table 14. Pin F6 of GEB-161 (at 11,722 MWd/kgU)**

Nuclide	HELIOS-1.4	HELIOS-1.6	HELIOS-1.6	Version 1.4 – 45 groups	Version 1.4
	34-group cross- section library	45-group cross- section library	190-group cross- section library		– 190 groups
	Atom density (atoms/barn·cm)	Atom density (atoms/barn·cm)	Atom density (atoms/barn·cm)		%
<sup>235</sup> U	4.252E-04	4.2318E-04	4.2328E-04	0.5	0.5
<sup>236</sup> U	2.846E-05	2.8665E-05	2.8537E-05	–0.7	–0.3
<sup>238</sup> U	2.145E-02	2.1460E-02	2.1460E-02	0.0	0.0
<sup>237</sup> Np	1.110E-06	1.2522E-06	1.2530E-06	–12.8	–12.9
<sup>239</sup> Pu	7.282E-05	6.9580E-05	6.8442E-05	4.4	6.0
<sup>240</sup> Pu	1.192E-05	1.1351E-05	1.1187E-05	4.8	6.1
<sup>241</sup> Pu	3.760E-06	3.4894E-06	3.6907E-06	7.2	1.8
<sup>242</sup> Pu	2.944E-07	2.7194E-07	2.9579E-07	7.6	–0.5
<sup>241</sup> Am	6.280E-08	5.7654E-08	6.2121E-08	8.2	1.1
<sup>243</sup> Am	1.341E-08	1.2921E-08	1.4497E-08	3.6	–8.1
<sup>242</sup> Cm	5.852E-09	5.3561E-09	5.7944E-09	8.5	1.0
<sup>243</sup> Cm+ <sup>244</sup> Cm	8.540E-10	8.2319E-10	9.2862E-10	3.6	–8.7
<sup>145</sup> Nd	6.095E-06	6.1072E-06	6.1131E-06	–0.2	–0.3
<sup>146</sup> Nd	5.048E-06	5.0568E-06	5.0647E-06	–0.2	–0.3
<sup>148</sup> Nd	2.878E-06	2.8781E-06	2.8821E-06	0.0	–0.1

**Table 15. Pin G1 of GEB-161 (at 11,722 MWd/kgU)**

Nuclide	HELIOS-1.4	HELIOS-1.6	HELIOS-1.6	Version 1.4 – 45 groups	Version 1.4 – 190 groups
	34-group cross- section library	45-group cross- section library	190-group cross- section library		
	Atom density (atoms/barn-cm)	Atom density (atoms/barn-cm)	Atom density (atoms/barn-cm)		
<sup>235</sup> U	1.602E-04	1.5768E-04	1.5763E-04	1.6	1.6
<sup>236</sup> U	3.674E-05	3.6968E-05	3.6913E-05	-0.6	-0.5
<sup>238</sup> U	2.243E-02	2.2431E-02	2.2431E-02	0.0	0.0
<sup>237</sup> Np	1.608E-06	1.6801E-06	1.6873E-06	-4.5	-4.9
<sup>239</sup> Pu	6.638E-05	6.4779E-05	6.4136E-05	2.4	3.4
<sup>240</sup> Pu	2.525E-05	2.4398E-05	2.4140E-05	3.4	4.4
<sup>241</sup> Pu	7.926E-06	7.6191E-06	7.7902E-06	3.9	1.7
<sup>242</sup> Pu	1.759E-06	1.6979E-06	1.7764E-06	3.5	-1.0
<sup>241</sup> Am	1.461E-07	1.3947E-07	1.4504E-07	4.5	0.7
<sup>243</sup> Am	1.135E-07	1.0937E-07	1.1794E-07	3.6	-3.9
<sup>242</sup> Cm	2.840E-08	2.7090E-08	2.8066E-08	4.6	1.2
<sup>243</sup> Cm+ <sup>244</sup> Cm	1.047E-08	1.0175E-08	1.1068E-08	2.8	-5.7
<sup>145</sup> Nd	1.028E-05	1.0286E-05	1.0303E-05	-0.1	-0.2
<sup>146</sup> Nd	8.974E-06	8.9915E-06	9.0123E-06	-0.2	-0.4
<sup>148</sup> Nd	5.090E-06	5.0903E-06	5.1022E-06	0.0	-0.2

Regarding changes from version 1.4 to 1.6 (first study), <sup>237</sup>Np inventories increased and most plutonium and trans-plutonium actinide inventories decreased. Regarding comparisons between the design and master libraries for version 1.6, for all of the MOX fuel pins, inventories of <sup>236</sup>U, <sup>243</sup>Am, and (<sup>242</sup>Cm + <sup>244</sup>Cm) as calculated with the master library are significantly greater than calculations performed with either the 34 or 45-group design libraries. For LEU fuels, significant discrepancies between the libraries (as much as 12%) exist for all transuranic actinides though these differences are nuclide dependent (some greater with version 1.6, some less).

#### **4. ABB-CE MIXED OXIDE ASSEMBLY WITH 24 $\text{UO}_2\text{-ER}_2\text{O}_3$ RODS**

Reference 6 provides documentation of studies of various ABB-Combustion Engineering (ABB-CE) pressurized-water-reactor MOX fuel assembly designs. A characteristic of these assembly designs that distinguishes them from other PWR assembly configurations is the use of uranium/erbium integral absorber rods in various locations within the 16 by 16 array of fuel pin locations (some locations are occupied by control rod tubes yielding a net number of rods/assembly of 236).

The results of these calculations are reported in Table 16. It was not possible to execute the input file with the 190 group library due to a lack of internal memory in the program. A “fix” was attempted by adding the OM option of the RUN operator in the input file but, unfortunately, success was not achieved.

Agreement between the two design libraries is generally within the 320 pcm value noted earlier in this report.

**Table 16. Comparison of multiplication factors for an ABB-CE MOX assembly**

Exposure (MWd/MT)	HELIOS-1.4 34-group cross-section library	HELIOS-1.6 45-group cross-section library	Difference
	$k_{inf}$	$k_{inf}$	%
0	1.23774	1.23596	0.14
50	1.21390	1.21231	0.13
500	1.20586	1.20431	0.13
1000	1.19885	1.19732	0.13
2000	1.18800	1.18649	0.13
3000	1.17897	1.17754	0.12
5000	1.16333	1.16204	0.11
7000	1.14891	1.14776	0.10
9000	1.13538	1.13433	0.09
11000	1.12251	1.12152	0.09
14000	1.10437	1.10337	0.09
17000	1.08682	1.08573	0.10
20000	1.06986	1.06858	0.12
23000	1.05334	1.05186	0.14
26000	1.03721	1.03547	0.17
30000	1.01649	1.01434	0.21
34000	0.99613	0.99353	0.26
38000	0.97633	0.97325	0.32
42000	0.95707	0.95358	0.36
46000	0.93838	0.93450	0.41
50000	0.92027	0.91606	0.46
54000	0.90275	0.89835	0.49
58000	0.88587	0.88130	0.52
62000	0.86960	0.86500	0.53
66000	0.85396	0.84947	0.53
70000	0.83899	0.83468	0.52
74000	0.82467	0.82063	0.49

## **5. WESTINGHOUSE $17 \times 17$ PRESSURIZED WATER REACTOR, MIXED OXIDE AND LOW-ENRICHED URANIUM (LEU) ASSEMBLIES**

Ref. 7 provides documentation of studies of various Westinghouse pressurized-water-reactor LEU and MOX fuel assembly designs. A characteristic of these assembly designs that distinguishes them from other PWR assembly configurations is the use of burnable absorber “finger rods” in control rod locations for some of those assemblies not located in control rod locations. Twenty-four absorber rods are located within the 17 by 17 array of fuel pin locations (the net number of fuel rods/assembly is 264). For LEU assemblies, some of the LEU pins may be coated with boron and serve as integral burnable absorber pins.

Calculations for an LEU assembly with 128 integral burnable absorber pins are reported in Table 17. Calculations for a MOX assembly with no integral burnable absorber pins are reported in Table 18.

Agreement among the MOX assembly calculations was excellent – well within the difference expected due to changes made by Studsvik/Scandpower. The perturbation in multiplication factor at 55,000 MWd/MT seen in the ABB-CE calculations is not apparent in the Westinghouse model.

The level of agreement among LEU calculations is poorer than that for MOX fuel. Discrepancies monotonically decrease with burnup. Only insignificant differences exist between the design and master libraries in version 1.6.

**Table 17. Comparison of multiplication factors for Westinghouse  $17 \times 17$  LEU assembly**

UO <sub>2</sub> 4.5 w/o with 128 IFBA	HELIOS1.4 34-group library	HELIOS1.4 89-group library	HELIOS1.6 45-group library	HELIOS1.6 190-group library	Version 1.4 34 – 45	Version 1.4 89 – 190
Exposure (MWd/MT)	$k_{inf}$	$k_{inf}$	$k_{inf}$	$k_{inf}$	%	%
0	1.13803	1.13734	1.13112	1.13119	0.61	0.54
500	1.11116	1.11060	1.10429	1.10450	0.62	0.55
1000	1.11524	1.11478	1.10851	1.10880	0.60	0.54
1500	1.12006	1.11964	1.11320	1.11353	0.61	0.55
2500	1.12813	1.12770	1.12102	1.12131	0.63	0.57
5000	1.13813	1.13740	1.13036	1.13033	0.68	0.62
7500	1.13840	1.13738	1.13007	1.12982	0.73	0.66
10000	1.13219	1.13098	1.12343	1.12309	0.77	0.70
12500	1.12171	1.12041	1.11267	1.11234	0.81	0.72
15000	1.10843	1.10713	1.09924	1.09900	0.83	0.73
17500	1.09332	1.09211	1.08412	1.08402	0.84	0.74
20000	1.07706	1.07599	1.06798	1.06801	0.84	0.74
22500	1.06013	1.05926	1.05125	1.05143	0.84	0.74
25000	1.04283	1.04219	1.03424	1.03458	0.82	0.73
27500	1.02536	1.02498	1.01712	1.01761	0.80	0.72
30000	1.00787	1.00776	1.00004	1.00068	0.78	0.70
35000	0.97362	0.97412	0.96675	0.96766	0.71	0.66
40000	0.93993	0.94105	0.93416	0.93527	0.61	0.61
45000	0.90728	0.90894	0.90266	0.90394	0.51	0.55
50000	0.87600	0.87815	0.87258	0.87397	0.39	0.48
55000	0.84644	0.84900	0.84423	0.84567	0.26	0.39
60000	0.81893	0.82177	0.81785	0.81932	0.13	0.30

**Table 18. Comparison of multiplication factors for Westinghouse  $17 \times 17$  MOX assembly**

MOX 4.5 w/o with 24 WABA	HELIOS1.4 34-group library	HELIOS1.6 45-group library	HELIOS1.6 190-group library	Version 1.4 34 – 45	Version 1.4 34 – 190
Exposure (MWd/MT)	$k_{inf}$	$k_{inf}$	$k_{inf}$	%	%
0	1.14457	1.1412	1.13854	0.29	0.53
500	1.11616	1.11292	1.11044	0.29	0.51
1000	1.10998	1.10673	1.10443	0.29	0.50
1500	1.10515	1.10194	1.09980	0.29	0.48
2500	1.09751	1.09439	1.09254	0.28	0.45
5000	1.08321	1.08045	1.07919	0.25	0.37
7500	1.07158	1.06914	1.06839	0.23	0.30
10000	1.06161	1.05943	1.05909	0.21	0.24
12500	1.05259	1.05065	1.05067	0.18	0.18
15000	1.04402	1.04225	1.04257	0.17	0.14
17500	1.03537	1.03377	1.03435	0.15	0.10
20000	1.02638	1.02491	1.02569	0.14	0.07
22500	1.01675	1.01539	1.01634	0.13	0.04
25000	1.00641	1.00514	1.00623	0.13	0.02
30000	0.98461	0.98346	0.98477	0.12	–0.02
35000	0.96041	0.95940	0.96081	0.11	–0.04
40000	0.93550	0.93462	0.93607	0.09	–0.06
45000	0.91095	0.91027	0.91171	0.07	–0.08
50000	0.88731	0.88687	0.88821	0.05	–0.10
55000	0.86484	0.86477	0.86603	0.01	–0.14
60000	0.84365	0.84407	0.84526	–0.05	–0.19





## 6. INFINITE ARRAYS OF VVER-1000 FUEL ASSEMBLIES

Several studies have been made of infinite arrays of VVER-1000 fuel assemblies (Ref. 8). The cases include an infinite array of high burnup LEU fuel (Variant 11), an infinite array of high burnup MOX fuel (Variant 12), an infinite array of a mixture of MOX and LEU with burnup but at room temperature conditions (Variant 14), and an infinite array of mixture of MOX and LEU at a temperature corresponding to accident conditions (Variant 20).

### 6.1. Variant 11, State 2, Burnup 60 MWd/kgU

Tables 19 through 24 provide a comparison of values from Ref. 8 with values from HELIOS-1.6. A comparison of pin power distribution is given in Fig. 1.

**Table 19. Values of  $k_{eff}$ ,  $k_0$ , and migration area**

	$k_{eff}$	$k_0$	$M^2$ (cm <sup>2</sup> )
HELIOS-1.4, 190 groups	0.5485	0.6534	61.01
HELIOS-1.6, 190 groups	0.5501	0.6553	60.985
Difference, %	+0.3	+0.3	-0.04

**Table 20. Cell macroscopic cross sections, flux, and flux ratios**

Parameter (see Ref. 8)	HELIOS-1.4			HELIOS-1.6 (190 groups)		
	Pin 1	Pin 29	Pin 72	Pin 1	Pin 29	Pin 72
$\Sigma_a$ (cm <sup>-1</sup> )	2.221E-02	1.929E-02	1.644E-02	2.2243E-02	1.9318E-02	1.6459E-02
$\Sigma_f$ (cm <sup>-1</sup> )	6.534E-03	5.720E-03	4.433E-03	6.5571E-03	5.7404E-03	4.4500E-03
$v\Sigma_f$ (cm <sup>-1</sup> )	1.829E-02	1.593E-02	1.238E-02	1.8359E-02	1.5981E-02	1.2432E-02
$\phi_{cell}$ (cm <sup>-2</sup> ·s <sup>-1</sup> )	6.309E+14	5.915E+14	5.343E+14	6.2842E+14	5.8926E+14	5.3243E+14
$\phi_{fuel} / \phi_{cell}$	1.0069	1.0057	1.0028	1.0069	1.0057	1.0028
$\phi_{clad} / \phi_{cell}$	1.001	1.0006	1.0004	1.0010	1.0006	1.0004
$\phi_{mod} / \phi_{cell}$	0.9954	0.9963	0.9981	9.9544E-01	9.9628E-01	9.9814E-01

**Table 20 (continued)**

	(Version 1.6 – 1.4)/Version 1.4 %		
	Pin 1	Pin 29	Pin 72
$\Sigma_a$ (cm <sup>-1</sup> )	+0.1	+0.1	+0.1
$\Sigma_f$ (cm <sup>-1</sup> )	+0.4	+0.4	+0.4
$\nu\Sigma_f$ (cm <sup>-1</sup> )	+0.4	+0.3	+0.4
$\phi_{\text{cell}}$ (cm <sup>-2</sup> ·s <sup>-1</sup> )	-0.4	-0.4	-0.3
$\phi_{\text{fuel}} / \phi_{\text{cell}}$	0	0	0
$\phi_{\text{clad}} / \phi_{\text{cell}}$	0	0	0
$\phi_{\text{mod}} / \phi_{\text{cell}}$	0	0	0

**Table 21. Cell relative absorption reaction rates**

Rel. Abs. Rate*	HELIOS-1.4			HELIOS-1.6 190 groups			(Version 1.4 – Version 1.6)/ Version 1.4 (%)		
(b)	Pin 1	Pin 29	Pin 72	Pin 1	Pin 29	Pin 72	1	29	72
<sup>235</sup> U	6.559E-02	7.800E-02	6.301E-02	6.5692E-02	7.8094E-02	6.3116E-02	-0.2	-0.1	-0.2
<sup>236</sup> U	1.122E-02	1.187E-02	1.330E-02	1.1204E-02	1.1853E-02	1.3281E-02	0.1	0.1	0.1
<sup>238</sup> U	2.763E-01	2.943E-01	3.363E-01	2.7588E-01	2.9389E-01	3.3580E-01	0.2	0.1	0.1
<sup>238</sup> Pu	4.100E-03	3.479E-03	3.348E-03	4.0548E-03	3.4332E-03	3.3015E-03	1.1	1.3	1.4
<sup>239</sup> Pu	2.381E-01	2.276E-01	2.029E-01	2.3898E-01	2.2864E-01	2.0389E-01	-0.4	-0.5	-0.5
<sup>240</sup> Pu	8.144E-02	7.939E-02	7.987E-02	8.1473E-02	7.9387E-02	7.9847E-02	0.0	0.0	0.0
<sup>241</sup> Pu	7.375E-02	6.681E-02	6.117E-02	7.3657E-02	6.6690E-02	6.1099E-02	0.1	0.2	0.1
<sup>242</sup> Pu	9.449E-03	8.688E-03	1.001E-02	9.3977E-03	8.6353E-03	9.9491E-03	0.5	0.6	0.6
<sup>135</sup> Xe	1.690E-02	1.574E-02	1.270E-02	1.6915E-02	1.5744E-02	1.2707E-02	-0.1	0.0	-0.1
<sup>149</sup> Sm	6.444E-03	6.036E-03	4.892E-03	6.4441E-03	6.0360E-03	4.8908E-03	0.0	0.0	0.0
FP	1.440E-01	1.380E-01	1.399E-01	1.4381E-01	1.3784E-01	1.3973E-01	0.1	0.1	0.1

\*Relative absorption rate is relative to the total corresponding reaction rate for the entire assembly.

**Table 22. Fuel-averaged microscopic absorption cross section**

Mic. Abs. X-Sec* (b)	HELIOS-1.4			HELIOS-1.6 190 groups			(Version 1.4 – Version 1.6)/ Version 1.4 (%)		
	Pin 1	Pin 29	Pin 72	Pin 1	Pin 29	Pin 72	1	29	72
<sup>235</sup> U	4.741E+01	3.849E+01	3.076E+01	4.7273E+01	3.8356E+01	3.0666E+01	0.3	0.3	0.3
<sup>236</sup> U	6.266E+00	5.745E+00	5.485E+00	6.2670E+00	5.7455E+00	5.4845E+00	0.0	0.0	0.0
<sup>238</sup> U	1.033E+00	9.527E-01	9.291E-01	1.0331E+00	9.5269E-01	9.2909E-01	0.0	0.0	0.0
<sup>238</sup> Pu	3.162E+01	2.527E+01	1.980E+01	3.1370E+01	2.5015E+01	1.9583E+01	0.8	1.0	1.1
<sup>239</sup> Pu	1.403E+02	1.123E+02	8.789E+01	1.3955E+02	1.1163E+02	8.7459E+01	0.5	0.6	0.5
<sup>240</sup> Pu	9.528E+01	7.948E+01	6.857E+01	9.3729E+01	7.8216E+01	6.7435E+01	1.6	1.6	1.7
<sup>241</sup> Pu	1.319E+02	1.052E+02	8.188E+01	1.3109E+02	1.0451E+02	8.1417E+01	0.6	0.7	0.6
<sup>242</sup> Pu	2.661E+01	2.495E+01	2.222E+01	2.6626E+01	2.4963E+01	2.2226E+01	-0.1	-0.1	0.0
<sup>135</sup> Xe	1.734E+05	1.312E+05	9.473E+04	1.7296E+05	1.3080E+05	9.4442E+04	0.3	0.3	0.3
<sup>149</sup> Sm	5.306E+03	4.049E+03	2.937E+03	5.2955E+03	4.0375E+03	2.9289E+03	0.2	0.3	0.3
FP	4.602E+00	4.102E+00	3.400E+00	4.6038E+00	4.1025E+00	3.4006E+00	0.0	0.0	0.0

\*Microscopic absorption cross section.

**Table 23. Cell relative production rates**

Rel. Prod. Rate (b)	HELIOS-1.4			HELIOS-1.6 190 groups			(Version 1.4 – Version 1.6)/ Version 1.4 (%)		
	Pin 1	Pin 29	Pin 72	Pin 1	Pin 29	Pin 72	1	29	72
<sup>235</sup> U	1.574E-01	1.850E-01	1.615E-01	1.5733E-01	1.8477E-01	1.6133E-01	0.0	0.1	0.1
<sup>236</sup> U	1.698E-03	1.944E-03	2.487E-03	1.6929E-03	1.9380E-03	2.4775E-03	0.3	0.3	0.4
<sup>238</sup> U	1.012E-01	1.181E-01	1.519E-01	1.0091E-01	1.1774E-01	1.5144E-01	0.3	0.3	0.3
<sup>238</sup> Pu	1.101E-03	1.095E-03	1.389E-03	1.0903E-03	1.0831E-03	1.3738E-03	1.0	1.1	1.1
<sup>239</sup> Pu	5.339E-01	5.082E-01	4.947E-01	5.3490E-01	5.0947E-01	4.9602E-01	-0.2	-0.2	-0.3
<sup>240</sup> Pu	2.003E-03	2.379E-03	3.060E-03	2.0328E-03	2.4124E-03	3.1039E-03	-1.5	-1.4	-1.4
<sup>241</sup> Pu	1.977E-01	1.789E-01	1.796E-01	1.9708E-01	1.7822E-01	1.7902E-01	0.3	0.4	0.3
<sup>242</sup> Pu	6.394E-04	6.401E-04	9.146E-04	6.3468E-04	6.3497E-04	9.0722E-04	0.7	0.8	0.8

\*Relative absorption rate is relative to the total corresponding production rate for the entire assembly.

**Table 24. Fuel-averaged microscopic production cross section**

Mic. Prod. X-Sec* (b)	HELIOS-1.4			HELIOS-1.6 190 groups			(Version 1.4 – Version 1.6)/ Version 1.6 (%)		
	Pin 1	Pin 29	Pin 72	Pin 1	Pin 29	Pin 72	1	29	72
<sup>235</sup> U	9.374E+01	7.535E+01	5.940E+01	9.3447E+01	7.5073E+01	5.9208E+01	0.3	0.4	0.3
<sup>236</sup> U	7.811E-01	7.766E-01	7.725E-01	7.8159E-01	7.7710E-01	7.7280E-01	-0.1	-0.1	0.0
<sup>238</sup> U	3.116E-01	3.155E-01	3.163E-01	3.1189E-01	3.1574E-01	3.1649E-01	-0.1	-0.1	-0.1
<sup>238</sup> Pu	6.997E+00	6.564E+00	6.188E+00	6.9619E+00	6.5284E+00	6.1549E+00	0.5	0.5	0.5
<sup>239</sup> Pu	2.592E+02	2.069E+02	1.615E+02	2.5780E+02	2.0577E+02	1.6071E+02	0.5	0.5	0.5
<sup>240</sup> Pu	1.930E+00	1.966E+00	1.980E+00	1.9303E+00	1.9662E+00	1.9800E+00	0.0	0.0	0.0
<sup>241</sup> Pu	2.911E+02	2.324E+02	1.812E+02	2.8949E+02	2.3103E+02	1.8019E+02	0.6	0.6	0.6
<sup>242</sup> Pu	1.483E+00	1.517E+00	1.530E+00	1.4842E+00	1.5185E+00	1.5308E+00	-0.1	-0.1	-0.1

\*Microscopic production cross section.

				0															
				0.773		0.776													
				0.703		0.703		0.696											
				0.692		0.698		0		0.685									
				0.729		0.738		0.704		0.694	0.726								
				0		0.752		0.720		0.720	0.739	0							
				0.906		0.840		0.810		0	0.809	0.835	0.906						
				1.074		1.014		0.966		0.904		0.903	0.965	1.012	1.074				
				1.171		1.126		1.092		1.054		1.048		1.054	1.091	1.125	1.170		
				1.224		1.193		1.169		1.146		1.134		1.134	1.145	1.169	1.192	1.224	
				1.286		1.256		1.239		1.220		1.208		1.204	1.208	1.221	1.239	1.256	1.286

				0																				
				0.774		0.777																		
				0.703		0.703		0.697																
				0.693		0.698		0		0.685														
				0.730		0.739		0.705		0.695		0.727												
				0		0.753		0.721		0.720		0.739		0										
				0.906		0.840		0.810		0		0.809		0.835		0.906								
				1.074		1.014		0.966		0.904		0.903		0.965		1.012		1.074						
				1.170		1.126		1.092		1.054		1.048		1.054		1.091		1.125		1.170				
				1.224		1.192		1.169		1.145		1.134		1.134		1.145		1.169		1.192		1.224		
				1.285		1.256		1.239		1.220		1.207		1.204		1.208		1.221		1.239		1.256		1.285

0  
0.13 0.13  
0 0 0.14  
0.14 0 0 0  
0.14 0.14 0.14 0.14 0.14  
0 0.13 0.14 0 0 0  
0 0 0 0 0 0 0  
0 0 0 0 0 0 0 0  
-0.09 0 0 0 0 0 0 0 0 0  
0 -0.08 0 0 -0.09 0 0 0 0 0 0  
-0.08 0 0 0 -0.08 0 0 0 0 0 0 -0.08

31

## 6.2 Variant 12, State 2, Burnup 60 MWd/kgU

Variant 12 is an infinite array of VVER assemblies fueled with mixed oxide. Tables 25 through 30 provide a comparison of values from Ref. 8 with values from HELIOS-1.6. A comparison of pin power distribution is given in Fig. 2.

**Table 25. Values of  $k_{eff}$ ,  $k_0$ , and migration area**

	$k_{eff}$	$k_0$	$cm^2$
HELIOS-1.4, 190 groups	0.5515	0.6550	59.92
HELIOS-1.6, 190 groups	0.5511	0.6544	59.88
Difference, %	-0.07	-0.09	-0.07

**Table 26. Cell macroscopic cross sections, flux, and flux ratios**

	HELIOS-1.4			HELIOS-1.6 190 groups		
	Pin 1	Pin 29	Pin 72	Pin 1	Pin 29	Pin 72
$\Sigma_a (cm^{-1})$	2.288E-02	2.001E-02	1.698E-02	2.2957E-02	2.0049E-02	1.7040E-02
$\Sigma_f (cm^{-1})$	6.442E-03	5.664E-03	4.388E-03	6.4474E-03	5.6650E-03	4.3943E-03
$v\Sigma_f (cm^{-1})$	1.859E-02	1.633E-02	1.265E-02	1.8613E-02	1.6338E-02	1.2667E-02
$\phi_{cell} (cm^{-2}\cdot s^{-1})$	6.315E+14	5.936E+14	5.394E+14	6.3052E+14	5.9285E+14	5.3911E+14
$\phi_{fuel} / \phi_{cell}$	1.0063	1.0053	1.0024	1.0063	1.0052	1.0024
$\phi_{clad} / \phi_{cell}$	1.0012	1.0007	1.0005	1.0012	1.0007	1.0005
$\phi_{mod} / \phi_{cell}$	0.9958	0.9965	0.9984	9.9576E-01	9.9654E-01	9.9835E-01

**Table 26 (continued)**

	(Version 1.6 – Version 1.4)/Version 1.6 (%)		
	Pin 1	Pin 29	Pin 72
$\Sigma_a (cm^{-1})$	+0.3	+0.2	+0.4
$\Sigma_f (cm^{-1})$	+0.08	+0.02	+0.14
$v\Sigma_f (cm^{-1})$	+0.1	+0.05	+0.1
$\phi_{cell} (cm^{-2}\cdot s^{-1})$	-0.2	-0.1	-0.05
$\phi_{fuel} / \phi_{cell}$	0	-0.01	0
$\phi_{clad} / \phi_{cell}$	0	0	0
$\phi_{mod} / \phi_{cell}$	0	0	0

**Table 27. Cell relative absorption reaction rates**

Rel. Abs. Rate* (b)	HELIOS-1.4			HELIOS-1.6 190 groups			(Version 1.6 – Version 1.4)/ Version 1.6 (%)		
	Pin 1	Pin 29	Pin 72	Pin 1	Pin 29	Pin 72	1	29	72
<sup>235</sup> U	3.647E-03	4.292E-03	3.545E-03	3.6266E-03	4.2690E-03	3.5259E-03	-0.6	-0.5	-0.5
<sup>236</sup> U	5.195E-04	5.526E-04	6.168E-04	6.0057E-04	6.3690E-04	7.0736E-04	+13.5	+13.2	+12.8
<sup>238</sup> U	2.685E-01	2.840E-01	3.265E-01	2.6695E-01	2.8251E-01	3.2439E-01	-0.6	-0.5	-0.6
<sup>238</sup> Pu	1.928E-03	1.682E-03	1.614E-03	1.9240E-03	1.6749E-03	1.6051E-03	-0.2	-0.4	-0.6
<sup>239</sup> Pu	2.474E-01	2.464E-01	2.142E-01	2.4685E-01	2.4599E-01	2.1388E-01	-0.2	-0.2	-0.1
<sup>240</sup> Pu	1.105E-01	1.134E-01	1.094E-01	1.0983E-01	1.1295E-01	1.0892E-01	-0.6	-0.4	-0.4
<sup>241</sup> Pu	1.150E-01	1.110E-01	9.871E-02	1.1430E-01	1.1045E-01	9.8192E-02	-0.6	-0.5	-0.5
<sup>242</sup> Pu	1.443E-02	1.340E-02	1.530E-02	1.7063E-02	1.5755E-02	1.7961E-02	+15.4	+14.9	+14.8
<sup>135</sup> Xe	1.600E-02	1.473E-02	1.194E-02	1.5933E-02	1.4663E-02	1.1875E-02	-0.4	-0.5	-0.5
<sup>149</sup> Sm	6.267E-03	5.842E-03	4.733E-03	6.2419E-03	5.8179E-03	4.7103E-03	-0.4	-0.4	-0.5
FP	1.497E-01	1.422E-01	1.466E-01	1.4875E-01	1.4135E-01	1.4557E-01	-0.6	-0.6	-0.7

\*Relative absorption rate is relative to the total corresponding reaction rate for the entire assembly.

**Table 28. Fuel-averaged microscopic absorption cross section**

Mic. Abs. X- Sec*	HELIOS-1.4			HELIOS-1.6 190 groups			(Version 1.6 – Version 1.4)/ Version 1.6 (%)		
	Pin 1	Pin 29	Pin 72	Pin 1	Pin 29	Pin 72	1	29	72
<sup>235</sup> U	4.217E+01	3.366E+01	2.754E+01	4.1975E+01	3.3490E+01	2.7421E+01	-0.5	-0.5	-0.4
<sup>236</sup> U	6.640E+00	6.221E+00	5.856E+00	7.9764E+00	7.4050E+00	6.9662E+00	+16.8	+16.0	+15.9
<sup>238</sup> U	1.028E+00	9.469E-01	9.256E-01	1.0248E+00	9.4373E-01	9.2283E-01	-0.3	-0.3	-0.3
<sup>238</sup> Pu	2.790E+01	2.189E+01	1.757E+01	2.7566E+01	2.1571E+01	1.7307E+01	-1.2	-1.5	-1.5
<sup>239</sup> Pu	1.221E+02	9.447E+01	7.581E+01	1.2119E+02	9.3772E+01	7.5307E+01	-0.7	-0.7	-0.7
<sup>240</sup> Pu	6.969E+01	5.427E+01	4.814E+01	6.9385E+01	5.4169E+01	4.8050E+01	-0.4	-0.2	-0.2
<sup>241</sup> Pu	1.149E+02	8.922E+01	7.114E+01	1.1410E+02	8.8582E+01	7.0692E+01	-0.7	-0.7	-0.6
<sup>242</sup> Pu	1.699E+01	1.612E+01	1.416E+01	2.1976E+01	2.0470E+01	1.8100E+01	+22.7	+21.3	+21.8
<sup>135</sup> Xe	1.479E+05	1.083E+05	7.968E+04	1.4704E+05	1.0748E+05	7.9131E+04	-0.6	-0.8	-0.7
<sup>149</sup> Sm	4.536E+03	3.350E+03	2.476E+03	4.5103E+03	3.3264E+03	2.4604E+03	-0.6	-0.7	-0.6
FP	4.829E+00	4.339E+00	3.622E+00	4.8156E+00	4.3230E+00	3.6093E+00	-0.3	-0.4	-0.4

\*Microscopic absorption cross section.

**Table 29. Cell relative production rates**

Rel. Prod. Rate*	HELIOS-1.4			HELIOS-1.6 190 groups			(Version 1.6 – Version 1.4)/ Version 1.6 (%)		
	Pin 1	Pin 29	Pin 72	Pin 1	Pin 29	Pin 72	1	29	72
<sup>235</sup> U	8.811E-03	1.020E-02	9.108E-03	8.7743E-03	1.0149E-02	9.0655E-03	-0.4	-0.5	-0.5
<sup>236</sup> U	7.740E-05	8.735E-05	1.120E-04	7.8175E-05	8.8288E-05	1.1250E-04	+1.0	+1.1	+0.4
<sup>238</sup> U	1.021E-01	1.181E-01	1.152E-01	1.0212E-01	1.1825E-01	1.5171E-01	+0.1	+0.1	0.0
<sup>238</sup> Pu	5.744E-04	5.980E-04	7.462E-04	5.7841E-04	6.0172E-04	7.5070E-04	-0.7	-0.6	-0.6
<sup>239</sup> Pu	5.621E-01	5.565E-01	5.284E-01	5.6227E-01	5.5656E-01	5.2867E-01	0.0	0.0	+0.1
<sup>240</sup> Pu	3.795E-03	5.073E-03	6.064E-03	3.8103E-03	5.0869E-03	6.0780E-03	+0.4	+0.3	+0.2
<sup>241</sup> Pu	3.128E-01	3.009E-01	2.938E-01	3.1165E-01	3.0018E-01	2.9288E-01	-0.4	-0.2	-0.3
<sup>242</sup> Pu	1.578E-03	1.572E-03	2.245E-03	1.4476E-03	1.4603E-03	2.0685E-03	-8.3	-7.1	-7.9

\*Relative absorption rate is relative to the total corresponding production rate for the entire assembly.



**Table 30. Fuel-averaged microscopic production cross section**

Mic. Prod. X- Sec*	HELIOS-1.4			HELIOS-1.6 190 groups			(Version 1.6 – Version 1.4)/ Version 1.6 (%)		
	Pin 1	Pin 29	Pin 72	Pin 1	Pin 29	Pin 72	1	29	72
<sup>235</sup> U	8.281E+01	6.528E+01	5.270E+01	8.2343E+01	6.4878E+01	5.2412E+01	-0.6	-0.6	-0.5
<sup>236</sup> U	8.041E-01	8.028E-01	7.921E-01	8.4184E-01	8.3647E-01	8.2362E-01	+4.5	+4.0	+3.8
<sup>238</sup> U	3.174E-01	3.215E-01	3.205E-01	3.1785E-01	3.2188E-01	3.2085E-01	+0.1	+0.1	+0.1
<sup>238</sup> Pu	6.757E+00	6.352E+00	6.050E+00	6.7194E+00	6.3149E+00	6.0172E+00	-0.6	-0.6	-0.5
<sup>239</sup> Pu	2.255E+02	1.742E+02	1.393E+02	2.2382E+02	1.7289E+02	1.3838E+02	-0.7	-0.8	-0.7
<sup>240</sup> Pu	1.946E+00	1.982E+00	1.988E+00	1.9517E+00	1.9879E+00	1.9933E+00	+0.3	+0.3	+0.3
<sup>241</sup> Pu	2.540E+02	1.976E+02	1.577E+02	2.5226E+02	1.9619E+02	1.5675E+02	-0.7	-0.7	-0.6
<sup>242</sup> Pu	1.510E+00	1.544E+00	1.548E+00	1.5117E+00	1.5461E+00	1.5497E+00	+0.1	+0.1	+0.1

\*Microscopic production cross section.

# HELIOS-1.4

0
0.788 0.790
0.714 0.714 0.705
0.702 0.706 0 0.692
0.736 0.748 0.711 0.700 0.733
0 0.756 0.726 0.725 0.742 0
0.904 0.839 0.810 0 0.809 0.834 0.903
1.075 1.014 0.967 0.901 0.900 0.966 1.012 1.074
1.169 1.125 1.092 1.054 1.048 1.054 1.091 1.125 1.169
1.219 1.189 1.167 1.144 1.133 1.133 1.144 1.166 1.189 1.219
1.276 1.248 1.232 1.215 1.202 1.199 1.203 1.215 1.232 1.248 1.276

## HELIOS-1.6, 190 group cross-section library

0
0.791 0.793
0.716 0.716 0.707
0.704 0.708 0 0.694
0.737 0.749 0.712 0.702 0.734
0 0.757 0.727 0.726 0.743 0
0.904 0.839 0.811 0 0.809 0.834 0.903
1.074 1.014 0.967 0.901 0.901 0.966 1.012 1.073
1.168 1.124 1.091 1.054 1.047 1.053 1.091 1.124 1.168
1.218 1.188 1.166 1.143 1.132 1.132 1.143 1.165 1.188 1.218
1.275 1.247 1.231 1.214 1.202 1.198 1.202 1.215 1.232 1.248 1.275

## Difference (Version 1.6 – Version 1.4)/Version 1.6 (%)

0
0.37 0.38
0.28 0.28 0.28
0.28 0.28 0 0.29
0.14 0.14 0.14 0.28 0.14
0 0.13 0.14 0.14 0.13 0
0 0 0.12 0 0 0 0
-0.09 0 0 0 0.11 0 0 -0.009
-0.09 -0.09 -0.09 0 -0.10 -0.09 0 -0.09 -0.0
-0.08 -0.08 -0.09 -0.09 -0.09 -0.09 -0.09 -0.09 -0.09 -0.08
-0.08 -0.08 -0.08 -0.08 0 -0.08 -0.08 0 0 0 -0.08

**Fig. 2. Cell relative fission rate distribution is relative to the total corresponding fission rate for the entire assembly. Variant 12, State 2, 60 Burnup MWd/kgU.**



# HELIOS-1.6, 190 group cross-section library

[illegible]

**Fig. 3 (continued)**

Percent difference (Version 1.6 – Version 1.4)/Version 1.6

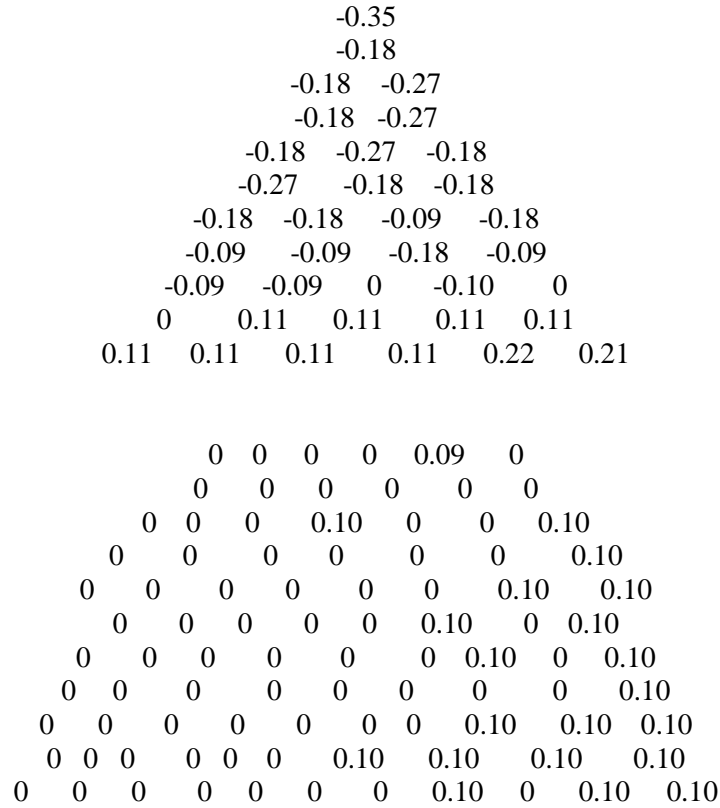


**Fig. 3 (continued)**

## 6.4 Variant 20, State 8

Variant 20 is an infinite array composed of irradiated UO<sub>2</sub> assemblies. In order to calculate the effective delayed neutron fraction, the required parameters have been commented out in both the HELIOS input file as well as in the zenith input file. When removing these comments, the 190 groups cross-section library required more internal memory than currently provided. Therefore, a calculation with 45 energy groups was executed to provide the results for the effective delayed neutron fraction. Results are provided in Table 31.

**Table 31. Delayed neutron fraction, effective delayed neutron fraction, and prompt neutron lifetime**

	Delayed neutron fraction	Effective delayed neutron fraction	Prompt neutron lifetime (sec)
HELIOS-1.4*	4.838E-03	4.645E-03	1.742E-05
HELIOS-1.6, 45 groups	4.8464E-03	4.9590E-03	1.5941E-05
HELIOS-1.6, 190 groups	4.8401E-03	N/A	1.5819E-05
Version 1.4 – 45 groups (%)	0.17	6.3	9.3
Version 1.4 – 190 groups (%)	0.04	N/A	10.1

\*Calculated with VENTURE (a reactor analysis system developed at ORNL); only HELIOS cross sections were used.

## 6.5. Conclusions

For the LEU assembly, changes from the 34-group version 1.4 calculation to the 190 group version 1.6 calculation were insignificant. It is postulated that the tighter pitch of the VVER assembly results in a faster neutron flux spectrum that, in turn, reduces the differences seen in previous sections of this report.

For VVER MOX assemblies, significant increases in  $^{236}\text{U}$  and  $^{242}\text{Pu}$  inventories are seen in the 190 group version 1.6 calculation as compared to the 34 group version 1.4 calculation. A significant reduction in prompt neutron lifetime in the mixed LEU/MOX “accident” model is also seen. Note that this is due to the fact that the VENTURE code was implemented in the HELIOS-1.4 results, while only HELIOS-1.6 was used for the version 1.6 results. While HELIOS can compute effective delayed neutron fractions via the BONE operator in ZENITH, this option uses the critical spectrum for the calculation. This is not consistent with the effective delayed neutron fraction required for the benchmark in Ref. 8. Therefore, HELIOS cross sections were implemented into the VENTURE code in order to compute the kinetics parameters for the benchmark calculations (Ref. 8). Consequently, the HELIOS-1.6 results do not match the HELIOS-1.4/VENTURE results since HELIOS-1.6 was only used for the version 1.6 results.

## 7. DESTRUCTIVELY ASSAYED VVER-1000 LEU ASSEMBLY

LEU assemblies were irradiated in a VVER-1000 reactor and subsequently destructively analyzed. The data are provided in Ref. 9. Computational results from this report, as well as the results of the HELIOS 1.6 calculations, are reported in Table 32.

The HELIOS input file is called bal3581.inp (for both the 45 groups and 190 groups cross-section libraries; the library names were changed in the input file for the two different calculations) and the output files are called bal3581\_45.hrf (45 groups) and bal3581.hrf (190 groups). The Zenith input files are z\_bal45.inp (45 groups) and z\_bal190.inp, (190 groups). The nuclides from the HELIOS output were in units of atoms/(barn ·cm) and had to be converted to mg/g UO<sub>2</sub> for comparison. Note that the uncertainties listed in Table 1 of report ORNL/TM-1999/168 are not included in Table 32 (applicable to the left-hand column).

For the 190 group calculations, the increases in the <sup>243</sup>Am and <sup>244</sup>Cm inventories with the version 1.6 190 group library are consistent with results of the LEU calculations for the Quad Cities reactor (Tables 14 and 15). A comparison of the 34 and 45-group calculations leads to discrepancies that are, in general, less than those seen for the Quad Cities reactor. Both the tighter pitch of the VVER and the higher burnup of the VVER rods relative to the Quad Cities rods could explain this phenomenon. The increase in the americium and curium inventories with version 1.6 results in better agreement with measured values as reported in Ref. 9.

**Table 32. Balakovo-3, Sample 581**

Nuclide	HELIOS-1.4 (mg/g UO <sub>2</sub> )	HELIOS-1.6 45 groups (mg/g UO <sub>2</sub> )	HELIOS-1.6 190 groups (mg/g UO <sub>2</sub> )	(45 groups – Version 1.4)/ 45 groups (%)	(190 groups – Version 1.4)/ 190 groups (%)
<sup>235</sup> U	8.7526	8.7218	8.7797	–0.4	–0.3
<sup>236</sup> U	5.8328	5.7198	5.6950	–1.9	–2.4
<sup>238</sup> U	925.66 (Ref. 9)	914.87	914.96	N/A	N/A
<sup>238</sup> Pu	0.2277	0.235	0.23365	+3.1	+2.5
<sup>239</sup> Pu	5.5328	5.6149	5.5226	+1.5	–0.2
<sup>240</sup> Pu	2.6532	2.5482	2.5097	–4.0	–5.4
<sup>241</sup> Pu	1.5488	1.5772	1.5808	+1.8	+2.0
<sup>242</sup> Pu	0.6864	0.6875	0.69592	+0.2	+1.4
<sup>241</sup> Am	0.04757	0.04944	0.050236	+3.8	+5.3
<sup>243</sup> Am	0.15168	0.15547	0.16285	+2.4	+6.9
<sup>242</sup> Cm	0.01978	0.02017	0.020364	+1.9	+2.9
<sup>244</sup> Cm	0.0553	0.05625	0.059276	+1.7	+6.7
<sup>142</sup> Nd	0.0333	0.032749	0.032551	–1.7	–2.2
<sup>143</sup> Nd	1.04405	1.0386	1.0403	–0.5	–0.4
<sup>144</sup> Nd	1.49226	1.4787	1.4773	–0.9	–1.0
<sup>145</sup> Nd	0.94044	0.92553	0.92518	–1.6	–1.6
<sup>146</sup> Nd	0.99693	0.98666	0.98749	–1.0	–0.9
Burnup	47.9 ± 0.7	47.35	47.37	–	–



## **8. CONCLUSIONS**

Quality assurance studies have been completed to enable the use of HELIOS version 1.6 and its two cross-section libraries for analyses associated with weapons-usable plutonium disposition in U.S. light water reactors and Russian VVER reactors. Changes in nuclide inventories are dependent on the system studied and the type of fuel. For selected actinides, the differences between the design library for version 1.4 and the master library for version 1.6 can be as high as 15%.



## 9. REFERENCES

1. R. T. Primm, III, J. D. Drischler, A. M. Pavlovichev, and Y. A. Styryne, *A Roadmap and Discussion of Issues for Physics Analyses Required to Support Plutonium Disposition in VVER-1000 Reactors*, ORNL/TM-2000/133, UT-Battelle, LLC, Oak Ridge National Laboratory, June 2000.
2. Scandpower, Inc., *HELIOS Documentation, FMS-The Scandpower Fuel Management System*, December 15, 1995.
3. R. E. MacFarlane and D. W. Muir, *The NJOY Nuclear Data Processing System, Version 91*, Los Alamos National Laboratory Report LA-12740-M, October 1994 (program documentation available as PSR-171 from Radiation Safety Information Computational Center, Oak Ridge National Laboratory, Oak Ridge, TN).
4. P. F. Rose and C. L. Dunford, Eds., "ENDF-102, Data Formats and Procedures for the Evaluated Nuclear Data File, ENDF-6," Brookhaven National Laboratory report BNL-NCS-44945 (July 1990).
5. S. E. Fisher and F. C. Difilippo, *Neutronics Benchmark for the Quad Cities-1 (Cycle 2) Mixed-Oxide Assembly Irradiation*, ORNL/TM-13567, Lockheed Martin Energy Research Corp., Oak Ridge National Laboratory, April 1998.
6. I. Ariane and P. J. Turinsky, *Evaluation of Mixed LEU-MOX Loading Patterns for LWRs Originating from Inability to Deliver MOX Assemblies (ABB-CE System 80 Reload Core Study)*, ORNL/SUB/99-19XSY063V-1, Lockheed Martin Energy Research Corp., Oak Ridge National Laboratory, February 1999.
7. G. Alonso-Vargas and M. L. Adams, *Studies of Flexible MOX/LEU Fuel Cycles*, ORNL/SUB/99-19XSY062V-1, Lockheed Martin Energy Research Corp., Oak Ridge National Laboratory, March 1999.
8. J. C. Gehin, C. Dourougie, M. B. Emmett, and R. A. Lillie, *Analysis of Weapons-Grade MOX VVER-1000 Benchmarks with HELIOS and KENO*, ORNL/TM-1999/78, Lockheed Martin Energy Research Corp., Oak Ridge National Laboratory, July 1999.
9. B. D. Murphy, J. Kravchenko, A. Lazarenko, A. Pavlovitchev, V. Sidorenko, and A. Chetveriko, *Simulation of Low-Enriched Uranium (LEU) Burnup in Russian VVER reactors with the HELIOS Code Package*, ORNL/TM-1999/168, Lockheed Martin Energy Research Corp., Oak Ridge National Laboratory, March 2000.



### INTERNAL DISTRIBUTION

- |                                    |   |
|------------------------------------|---|
| 1. B. B. Bevard, 9104-1, MS-8057   | 15. G. E. Michaels, 9201-3, MS-8063                 |
| 2. B. L. Broadhead, 6011, MS-6370  | 16. M. P. McGinnis, 9201-3, MS-8065                 |
| 3. S. M. Bowman, 6011, MS-6370     | 17. B. D. Murphy, 6011, MS-6370                     |
| 4. W. C. Carter, 6011, MS-6370     | 18. C. V. Parks, 6011, MS-6370                      |
| 5. M. D. DeHart, 6011, MS-6370     | 19. L. M. Petrie, 6011, MS-6370                     |
| 6. F. C. Difilippo, 6025, MS-6363  | 20-24. R. T. Primm III, 6025, MS-6363               |
| 7. R. J. Ellis, 6025, MS-6363      | 25. B. T. Rearden, 6011, MS-6370                    |
| 8. M. B. Emmett, 6011, MS-6370     | 26. C. E. Sanders, 6011, MS-6370                    |
| 9. S. E. Fisher, 9104-1, MS-8057   | 27. D. J. Spellman, 9104-1, MS-8057                 |
| 10. I. C. Gauld, 6011, MS-6370     | 28. J. C. Wagner, 6011, MS-6370                     |
| 11. J. C. Gehin, 6025, MS-6363     | 29. ORNL Central Research Library<br>4500N, MS-6191 |
| 12. S. R. Greene, 9104-1, MS-8057  | 30. ORNL Laboratory Records-RC<br>4500N, MS-6254    |
| 13. D. T. Ingersoll, 6025, MS-6363 |   |
| 14. M. A. Kuliasha, 6025, MS-6435  |   |

### EXTERNAL DISTRIBUTION

31. M. L. Adams, Department of Nuclear Engineering, Texas A&M University, Zachry 129, College Station, TX 77843
32. D. Alberstein, Los Alamos National Laboratory, MS-K551, P.O. Box 1663, Los Alamos, NM 87545
33. Dr. Kiyonori Aratani; Surplus Weapons Plutonium Disposition Group; International Cooperation and Nuclear Material Control Division; Japan Nuclear Cycle Development Institute; 4-49 Muramatsu, Tokai-mura, Naka-gun, Ibaraki-ken, Japan
34. J. Baker, Office of Fissile Materials Disposition, U.S. Department of Energy, NN-63, 1000 Independence Avenue SW, Washington, DC 20585
35. J. B. Briggs, Idaho National Environmental and Engineering Laboratory, P.O. Box 1625-3855, Idaho Falls, ID 83415-3855
36. A. K. Caponiti, Office of Fissile Materials Disposition, U.S. Department of Energy, NN-63, 1000 Independence Avenue SW, Washington DC 20585
37. B. N. Fletcher, Office of Fissile Materials Disposition, U.S. Department of Energy, NN-63, 1000 Independence Avenue SW, Washington DC 20585
38. M. S. Chatterton, U.S. Nuclear Regulatory Commission, NRR/DSSA/SRXB, MS O10 B3, Washington, D.C. 20555-0001
39. C. K. Chidester, Los Alamos National Laboratory, MS-E502, P.O. Box 1663, Los Alamos, NM 87545

40. R. H. Clark, Duke Cogema Stone & Webster, 400 South Tryon Street, WC-32G, P.O. Box 1004, Charlotte, NC 28202
41. D. W. Danker, U.S. Department of Energy, NN-62, 1000 Independence Avenue SW, Washington DC 20585
42. A. Ferri; Scandpower, Inc., 101 Lakeforest Blvd., Suite 340, Gaithersburg, MD 20877
43. E. T. Gould, Lawrence Livermore National Laboratory, P.O. Box 808, MS-L186, Livermore, CA 94551
44. L. Jardine, Lawrence Livermore National Laboratory, P.O. Box 808, MS-L166, Livermore, CA 94551
- 45–49. Dr. Alexander Kalashnikov, Institute of Physics and Power Engineering, 1 Bondarenko Square, Obninsk, Kaluga Region, Russia 249020
50. R. Y. Lee, U.S. Nuclear Regulatory Commission, RES/DSARE/SMSAB, MS O10 B3, Washington, D.C. 20555-0001
51. S. Nesbit, Duke Cogema Stone & Webster, 400 South Tryon Street, WC-32G, P.O. Box 1004, Charlotte, NC 28202
52. J. O. Nulton, Office of Fissile Materials Disposition, U.S. Department of Energy, NN-61, 1000 Independence Avenue SW, Washington, DC 20585
- 53–54. Office of Scientific and Technical Information, U.S. Department of Energy, P.O. Box 62, Oak Ridge, TN 37831
55. Nagao Ogawa; Director and General Manager; Plant Engineering Department; Nuclear Power Engineering Corporation; Shuwa-Kamiyacho Building, 2F; 3-13, 4-Chome Toranomon; Minato-Ku, Tokyo 105-0001, Japan
56. Dr. S. L. Passman, Booz-Allen & Hamilton, 555 13<sup>th</sup> Street, NW, #480E, Washington, D.C. 20004
- 57–61. Dr. Alexander Pavlovitchev, Russian Research Center “Kurchatov Institute,” Institute of Nuclear Reactors, VVER Division, VVER Physics Department, 123182, Kurchatov Square, 1, Moscow, Russia
62. P. T. Rhoads, Office of Fissile Materials Disposition, U.S. Department of Energy, NN-61, 1000 Independence Avenue SW, Washington, DC 20585
63. U. Shoop, U.S. Nuclear Regulatory Commission, NRR/DSSA/SRXB, MS O10 B3, Washington, D.C. 20555-0001
64. E. Siskin, Office of Fissile Materials Disposition, U.S. Department of Energy, NN-60, 1000 Independence Avenue SW, Washington DC 20585
65. J. Thompson, Office of Fissile Materials Disposition, U.S. Department of Energy, NN-61, 1000 Independence Avenue SW, Washington, DC 20585
66. F. Trumble, Westinghouse Savannah River Company, Building 730R, Room 3402, WSRC, Aiken, SC 29808